

Spin-dependent Fano resonance induced by conducting chiral helimagnet contained in a quasi-one-dimensional electron waveguide

Rui Zhu^{*}

*Department of Physics, South China University of Technology,
Guangzhou 510641, People's Republic of China*

Abstract

Fano resonance appears for conduction through an electron waveguide containing donor impurities. In this work, we consider the thin-film conducting chiral helimagnet (CCH) as the donor impurity in a one-dimensional waveguide model. Due to the spin spiral coupling, interference between the direct and intersubband transmission channels gives rise to spin-dependent Fano resonance effect. The spin-dependent Fano resonance is sensitively dependent on the helicity of the spiral. By tuning the CCH potential well depth and the incident energy, this provides a potential way to detect the spin structure in the CCH.

PACS numbers: 85.75.-d, 75.30.Et, 72.10.Fk

^{*} Corresponding author. Electronic address: rzhu@scut.edu.cn

I. INTRODUCTION

Fano resonance, characterized by resonant reflection results from constructive and destructive interference of two quantum paths across localized and extended states¹⁻³. It is a universal effect existing almost in all interfering quantum processes independent of the specific details of the system under study. The interfering paths can be formed by spatial inhomogeneity as well as time-dependent oscillation. Subsequent to its discovery, there have been a great number of studies devoted to Fano resonances in various quantum systems, such as Anderson impurity systems⁴, quantum dots^{5,6}, scattering from a donor impurity in an electron waveguide,^{2,7} tunneling through an $\text{Al}_x\text{Ga}_{1-x}\text{As}$ barrier^{2,8}, transmission through a waveguide linked to a resonant cavity^{2,9}, nanowires and tunnel junctions¹⁰ and etc.³. Recently, the Fano resonance has been found¹¹ in plasmonic nanoparticles, photonic crystals, and electro magnetic metamaterials. The steep dispersion of the Fano resonance profile promises applications in sensors, lasing, switching, and nonlinear and slow-light devices¹¹.

Chiral helimagnets are static magnetic states sustained in various materials lacking rotoinversion symmetry with Dzyaloshinskii-Moriya (DM) antisymmetric exchange interaction¹². It is also the ground magnetic structure of most multiferroic materials. Recently, the spatial-dependent spin structure were exploited in different functional devices such as persistent spin currents¹³, spin-field-effect transistor¹⁴, tunneling anisotropic magnetoresistance¹⁵, spin resonance¹² and spin diffraction¹⁶⁻¹⁸. It has been shown that different transverse tunnels of transmission are coupled by a helimagnetic layer inserted between two free-electron layers¹⁶⁻¹⁸. A possible experimental candidate of a conducting chiral helimagnet (CCH)¹⁹, where free electrons are coupled with the background helimagnetic texture via the sd-type interaction is currently available in¹⁹, $\text{Cr}_{1/3}\text{NbS}_2$. Based on these observations, we consider a quasi-one-dimensional wave guide containing a thin CCH well and investigate the transport properties in it. The sd-exchange couples the free-electron spin with the spiral spin texture giving rise to a prominent Fano effect. In the electron waveguide configuration, Fano conductance is sensitively dependent on the CCH helicity, which provides a potential measurement of the spin spiral structure in the CCH.

II. THEORETICAL FORMULATION

The device we propose is a quasi-1D electron waveguide embedded with a thin layer of CCH acting as a donor impurity, which is depicted in Fig. 1. The Schrödinger equation describing scattering in such a device is

$$[-\nabla^2 + V_c(x) + V_{sc}(x, z)] \psi(x, z) = E\psi(x, z). \quad (1)$$

Confining potential $V_c(x)$ of the wave guide is an infinite square well across the x -direction, with eigenstates $\phi_n(x) = \sqrt{2/a} \sin(n\pi x/a)$ and corresponding subband energies $\varepsilon_n = \hbar^2 \pi^2 n^2 / 2ma^2$ with n the subband index and m the free-electron mass. We consider an ultrathin CCH layer, that is, the localized spin-dependent scattering potential can be approximated by a Dirac-delta function as

$$V_{sc}(x, z) = \left(\tilde{J} \mathbf{n}_r \cdot \sigma - V_0 d \right) \delta(z), \quad (2)$$

where \tilde{J} is the sd-type exchange coupling strength between free electrons and the background spin texture, $\mathbf{n}_r = [\sin \bar{q}x, 0, \cos \bar{q}x]$ is the local magnetization direction with $\bar{q} = 2\pi/\lambda$ the spin wave vector of the spiral (λ is the spiral period), σ is the Pauli vector, and V_0 and d are depth and width of the potential well, respectively. Here we consider $\lambda = a/2, a, 2a, 4a$, and $6a$.

Using the waveguide eigenstates $\{\phi_n\}$ as the expanding basis of the wave function $\psi(x, z)$, Eq. (1) can be converted to a set of linear equations. In the matrix formulism, the equations are^{2,20}

$$[-2iK_{mn}^{\alpha\beta} + V_{mn}^{\alpha\beta}] T_{nl}^{\beta\gamma} = -2iK_{ml}^{\alpha\gamma}, \quad (3)$$

where $K_{mn}^{\alpha\beta} = k_m \delta_{mn} \otimes I_{\alpha\beta}$ is elements of the diagonal matrix of wave vectors with $k_m = \sqrt{E - \varepsilon_m}$ and is extended to the wave-spin product space. Also, elements of the spin-dependent interband transition matrix

$$V_{mn}^{\alpha\beta} = \langle \phi_m^\alpha | \left(\tilde{J} \mathbf{n}_r \cdot \sigma + V_0 d \right) | \phi_n^\beta \rangle, \quad (4)$$

where

$$|\phi_m^\uparrow\rangle = \psi_m \otimes \begin{pmatrix} 1 \\ 0 \end{pmatrix}, \quad |\phi_m^\downarrow\rangle = \psi_m \otimes \begin{pmatrix} 0 \\ 1 \end{pmatrix}, \quad (5)$$

expressed in the σ_y representation. In Eq. (3) Einstein notation is employed with the upper and lower footnotes indexing the spin and subband elements respectively. Therefore,

the spin-dependent transmission amplitudes $T_{nl}^{\beta\gamma}$ can be obtained from Eq. (3) by matrix algebra. Here $T_{nl}^{\beta\gamma}$ denotes transmission amplitudes from the l -th subband with spin- γ polarization to the n -th subband with spin- β polarization. And the spin-dependent conductance can be calculated from the two-terminal Landauer formula²,

$$G_\alpha = \frac{e^2}{h} \sum_{mn\beta} \left(\frac{k_m}{k_n} \right) T_{mn}^{*\alpha\beta} T_{mn}^{\alpha\beta}, \quad (6)$$

where α indexes the spin-up or down channel and the m and n are summed only over the propagating modes.

III. NUMERICAL RESULTS AND INTERPRETATIONS

We consider the transmission properties of the CCH-layer-embedded quasi-1D electron waveguide. In numerical calculations, the sd-exchange coupling strength $\tilde{J} = 200 \text{ meV} \cdot \text{nm}$, which is reasonable compared to other energy scales in the considered system. In our model, the width of the waveguide $a = 5 \text{ nm}$ and the CCH spiral period λ varies with skipped values from $a/2$ to $6a$ with the spiral vector $\bar{q} = 2\pi/\lambda$. Namely, $\lambda = 2.5 \text{ nm}$ to 30 nm , which are typical values from experiment observation²¹. Potential well width of the CCH plane $d = 2 \text{ nm}$ and the potential well depth can be continuously tuned by gate voltages applied on the CCH layer.

We set the incident energy E between the first and second subbands of the waveguide with the eigen-energies $\varepsilon_1 \approx 15$ and $\varepsilon_2 \approx 60 \text{ meV}$. When the lateral width of the waveguide is small giving rise to large energy spacing between subbands, the two-subband cutoff is an acceptable approximation. Thus we neglect all but the first and second subbands and solve the resulting 4×4 matrix equation. So that the only incident wave is in the lowest subband with either spin component.

When a spiral helimagnet layer, conducting or insulating, is contained in a 2D waveguide or in free space transport, spin-dependent diffraction can be seen^{16–18}, i.e., spin-spiral wave vectors are added to or subtracted from the incident momentum wave vector and the electron is diffracted to different directions with spin reoriented. However, in a quasi-1D waveguide, diffraction is not sustained due to mode connection on the two sides of the CCH layer. In this situation, spin-dependent interband transition produces interference between direct and intersubband transmission channels resulting in the Fano resonance.

Numerical results of the transmission are given in Figs. 2 to 5. As the inter-subband scattering potential acts in the spin space, difference between the spin-conserved and spin-flipped transmission is prominent. Spin polarization of the incident electron depends on the reservoirs at the ends of the waveguide. In our approach, σ_y -representation is used, which gives rise to spin-up and down symmetry in all the transmissions, i.e. $T^{\uparrow\uparrow} = T^{\downarrow\downarrow}$ and $T^{\uparrow\downarrow} = T^{\downarrow\uparrow}$. In more formulation detail, the matrix scattering potential in the spin space

$$\tilde{J}\mathbf{n}_r \cdot \boldsymbol{\sigma} + V_0d = \begin{pmatrix} V_0d & \tilde{J}(\cos \bar{q}x - i \sin \bar{q}x) \\ \tilde{J}(\cos \bar{q}x + i \sin \bar{q}x) & V_0d \end{pmatrix}, \quad (7)$$

which is hermitian. This symmetry would be modified when the incident spin polarization is not (anti)parallel to the y -direction.

It is known that the transmission probability of a waveguide embedded with a plane δ -potential well or barrier is $4k_1^2/(4k_1^2 + V_0d)$ without resonance or antiresonance. With spatially-modulated δ -potential scattering, the lowest evanescent mode is correlated with the propagating mode. Interference between the direct tunneling path and that through inter-subband scattering gives rise to resonant or antiresonant transmission. In our considered structure, the scattering potential acts in the spin space. Both the spin-conserved and flipped transmission demonstrates resonance or antiresonance at certain incident energy and CCH-well depth. Diagonal elements of the transition matrix $V_{mn}^{\alpha\beta}$ are V_0d while the cross elements depends on the CCH spiral structure. The potential well depth and the inter-band scattering strength coact to the transmission probability. For all the spiral structure considered, resonance or Fano resonance can be found at certain V_0 and E parameter set up.

Figs. 2 to 5 are transmission results for different spiral periods. For $\lambda = 2a$, resonant tunneling occurs for spin-conserved transmission and standard Fano resonance occurs for spin-flipped transmission. In this configuration, only a half spiral period is within the waveguide. When the scattering potential sinusoidally varies in space, coincidence exists between the waveguide mode and that potential. When the potential cosinusoidally varies in space, coincidence does not appear between the waveguide mode and that potential. As a result, Fano resonance is not found in spin-conserved transmission.

For $\lambda = 4a$ and $6a$, only $1/4$ and $1/6$ of the spiral period are within the waveguide, respectively. Geometry of the scattering potential "seen" by the transporting electron includes different waveguide modes. Complete reflection occurs for both spin-conserved and flipped

transmission, which indicates a Fano resonance. As the spiral period increases difference between different λ becomes less prominent.

$\lambda = a$ is a special case as the spiral period equals the waveguide width. The x -component of the magnetization spirals sinusoidally and the z -component of the magnetization spirals cosinusoidally in space. The sinusoidal component of the spin spiral $\sin \bar{q}x$ coincides with the second waveguide mode $\phi_2(x) = \sqrt{2/a} \sin(2\pi x/a)$. As a result, spin-flipped transmission is dramatically suppressed demonstrating approximate complete reflection in all parameter regimes. And spin-conserved transmission demonstrates slow-varying antiresonance without considerable resonance. This can be explained by strong path interference of the tunneling process.

The case is different for $\lambda = a/2$. There are two spiral periods within the waveguide. The spiral variation $\sin \bar{q}x$ coincides with higher waveguide mode $\phi_4(x) = \sqrt{2/a} \sin(4\pi x/a)$. The eigenenergy of this mode $\varepsilon_4 \approx 241$ meV is far away from the first and second mode energy, thus contributes little to interband transition and are neglected. Spin-conserved transmission demonstrates an antiresonance and spin-flipped transmission demonstrates a resonance.

For all the spiral periods, resonance peak in spin-conserved transmission occurs exactly at the energy of the antiresonance valley in spin-flipped transmission and vice versa. This can be interpreted by the scatterer profile. The sinusoidally-space-dependent spin exchange coupling coacts with the δ -potential-well. Without the exchange coupling, transmission through a δ -well in a waveguide varies monotonously in the E - V_0 parameter plane. The spin exchange coupling modulates this transmission probability in the spin space. Namely, the plane δ -well transmission is enveloped by that modulation in spin space. The total transmission including both the spin-conserved and spin-flipped one is that of a plane δ -well. That beam of spin-up incidence is split with spin-up wave transmitted and spin-down wave reflected. In this way, the CCH spiral also works as a spin splitter with fixed spiral period and potential well depth.

Numerical results of the conductance are given in Fig. 6. Due to σ - y symmetry of the spiral and our representation setup, conductance in the spin-up channel G^\uparrow equals that in the spin-down channel G^\downarrow . It can be seen that spin-conserved transmission dominates the conductance. This is an effect of spiral chirality of the CCH. There would be one spin dominance for a particular spin handedness or chirality analogous to circularly-polarized light

traversing a spiral grating²². We used right-handed spiral CCH throughout our calculation, which gives rise to the spin-conserved transmission dominance. It can be seen that the conductance sensitively depends on the spiral structure of the CCH, which may lend a potential way to measure the magnetization configuration of certain materials.

IV. CONCLUSIONS

Spin-dependent Fano resonance in a CCH-film-embedded quasi-1D electron waveguide was investigated. The CCH layer acts as a donor impurity with sinusoidally-space-dependent spin-exchange coupling. From numerical results of the transmission and conductance for different CCH spiral periods λ , it was found that the transport probabilities differ conspicuously for different relation between λ and the waveguide width a . It was also found that by tuning the CCH potential well depth, transmission varies with spin-conserved and spin-flipped resonant or anti-resonant tunneling occurring at different incident electron energy. The proposed device may have potential application in spintronics and spiral magnetization determination.

V. ACKNOWLEDGEMENTS

The author acknowledges enlightening discussions with Zhi-Lin Hou, Wen-Ji Deng, and Jamal Berakdar. This project was supported by the National Natural Science Foundation of China (No. 11004063) and the Fundamental Research Funds for the Central Universities, SCUT (No. 2012ZZ0076).

-
- ¹ U. Fano, Phys. Rev. **124**, B1866 (1961).
- ² E. Tekman and P. F. Bagwell, Phys. Rev. B **48**, 2553 (1993).
- ³ A. E. Miroshnichenko, S. Flach, Y. S. Kivshar, Rev. Mod. Phys. **82**, 2257 (2010).
- ⁴ H. G. Luo, T. Xiang, X. Q. Wang, Z. B. Su, and L. Yu, Phys. Rev. Lett. **92**, 256602 (2004).
- ⁵ A. C. Johnson, C. M. Marcus, M. P. Hanson, and A. C. Gossard, Phys. Rev. Lett. **93**, 106803 (2004).
- ⁶ B. R. Bulka and P. Stefański, Phys. Rev. Lett. **86**, 225128 (2001).
- ⁷ C. S. Chu and R. S. Sorbello, Phys. Rev. B **40**, 5941 (1989).
- ⁸ T. B. Boykin, B. Pezeshki, and J. S. Harris, Phys. Rev. B **46**, 12769 (1992).
- ⁹ W. Porod, Z. Shao, and C. S. Lent, Appl. Phys. Lett. **61**, 1350 (1992).
- ¹⁰ K. Kobayashi, H. Aikawa, A. Sano, S. Katsumoto, and Y. Iye, Phys. Rev. B **70**, 035319 (2004).
- ¹¹ B. Lukyanchuk, N. I. Zheludev, S. A. maier, N. J. Halas, P. Nordlander, H. Giessen, and C. T. Chong, Nature Materials **9**, 707 (2010).
- ¹² J. I. Kishine and A. S. Ovchinnikov, Phys. Rev. B **79**, 220405(R) (2009).
- ¹³ J. Heurich, J. König, and A. H. MacDonald, Phys. Rev. B **68**, 064406 (2003).
- ¹⁴ C. Jia and J. Berakdar, Appl. Phys. Lett. **95**, 012105 (2009).
- ¹⁵ C. Jia and J. Berakdar, Phys. Rev. B **81**, 052406 (2010).
- ¹⁶ A. Manchon, A. Pertsova, N. Ryzhanova, A. Vedyayev, and B. Dieny, J. Phys.: Condens. Matter **20**, 505213 (2008).
- ¹⁷ A. Manchon, N. Ryzhanova, A. Vedyayev, and B. Dieny, J. Appl. Phys. **103**, 07A721 (2008);
- ¹⁸ R. Zhu, arXiv:1204.6095.
- ¹⁹ J. I. Kishine, I. V. Proskurin, and A. S. Ovchinnikov, Phys. Rev. Lett. **107**, 017205 (2011).
- ²⁰ P. F. Bagwell, Phys. Rev. B **41**, 10354 (1990).
- ²¹ N. Kanazawa, Y. Onose, T. Arima, D. Okuyama, K. Ohoyama, S. Wakimoto, K. Kakurai, S. Ishiwata, and Y. Tokura, Phys. Rev. Lett. **106**, 156603 (2011).
- ²² K. A. Bachman, J. J. Peltzer, P. D. Flammer, T. E. Furtak, R. T. Collins, and R. E. Hollingsworth, Optics Express **20**, 1308 (2012).

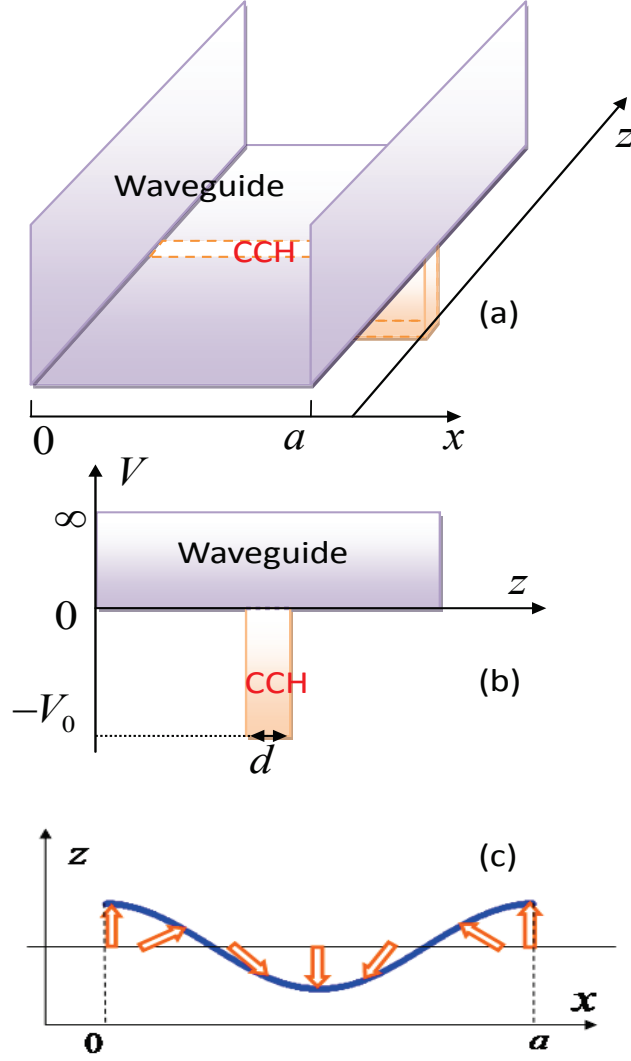


FIG. 1: Schematics of the proposed device. As shown in panel (a), propagation direction of the quasi-1D waveguide is in the z -coordinate with lateral width a and infinite confining potential. Panel (b) is the side intersection of the energy profile. The conducting chiral helimagnet (CCH) layer has thickness d and potential-well-depth V_0 . The spiral spin structure of the CCH is sketched in panel (c). The spin in one atomic layer of the x - y plane spirals in the x -direction with the local magnetization direction $\mathbf{n}_r = [\sin \bar{q}x, 0, \cos \bar{q}x]$, where $\bar{q} = 2\pi/a$ is the spin wave vector of the spiral.

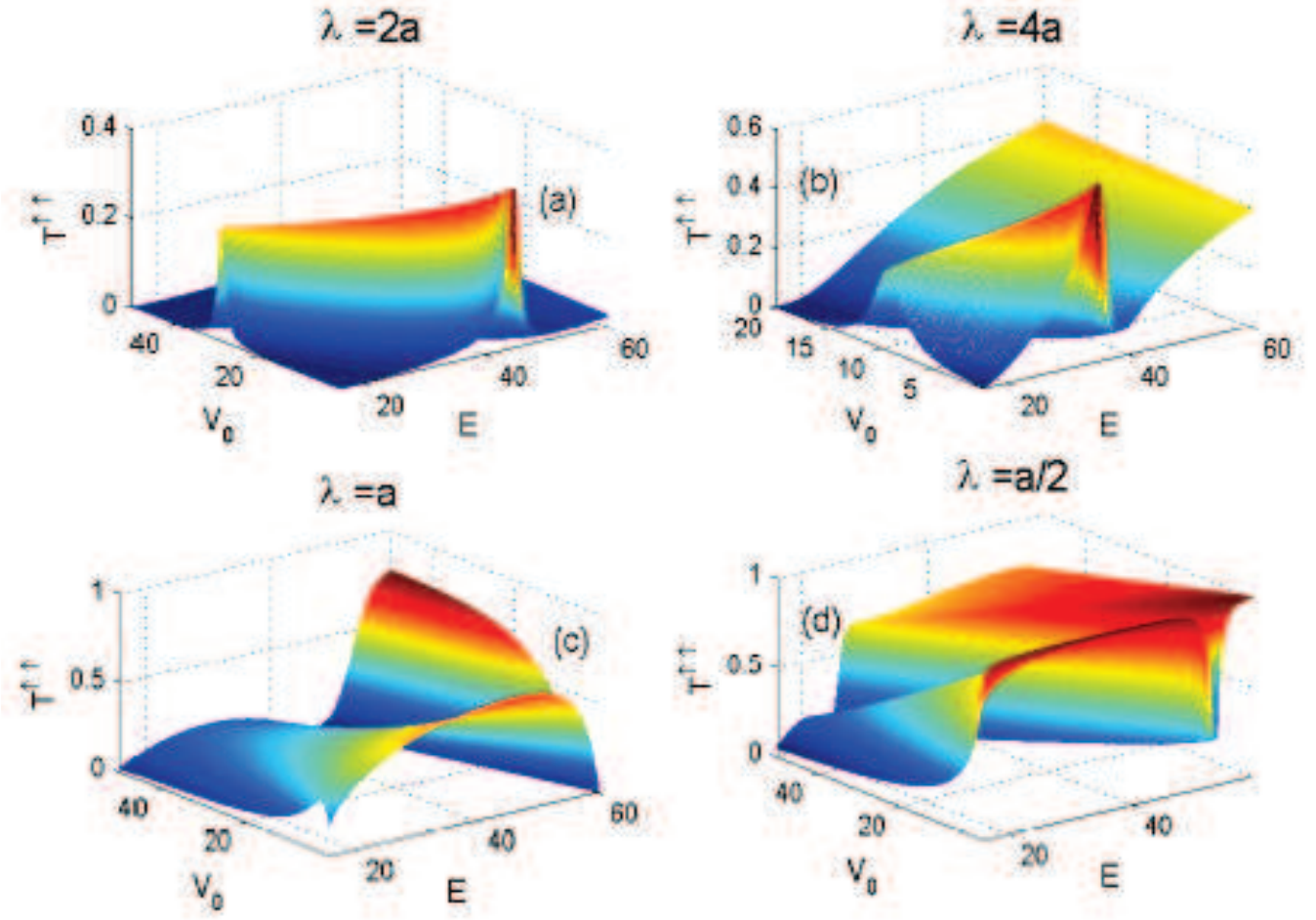


FIG. 2: Spin-conserved transmission $T^{\uparrow\uparrow}$ as a function of the incident energy E and the CCH well depth V_0 in the CCH-film-embedded quasi-1D electron waveguide. The four panels are for different spiral periods λ . As discussed in the text, only the propagating subband (the first one) is considered. Here, $T^{\uparrow\uparrow} = T^{\downarrow\downarrow}$.

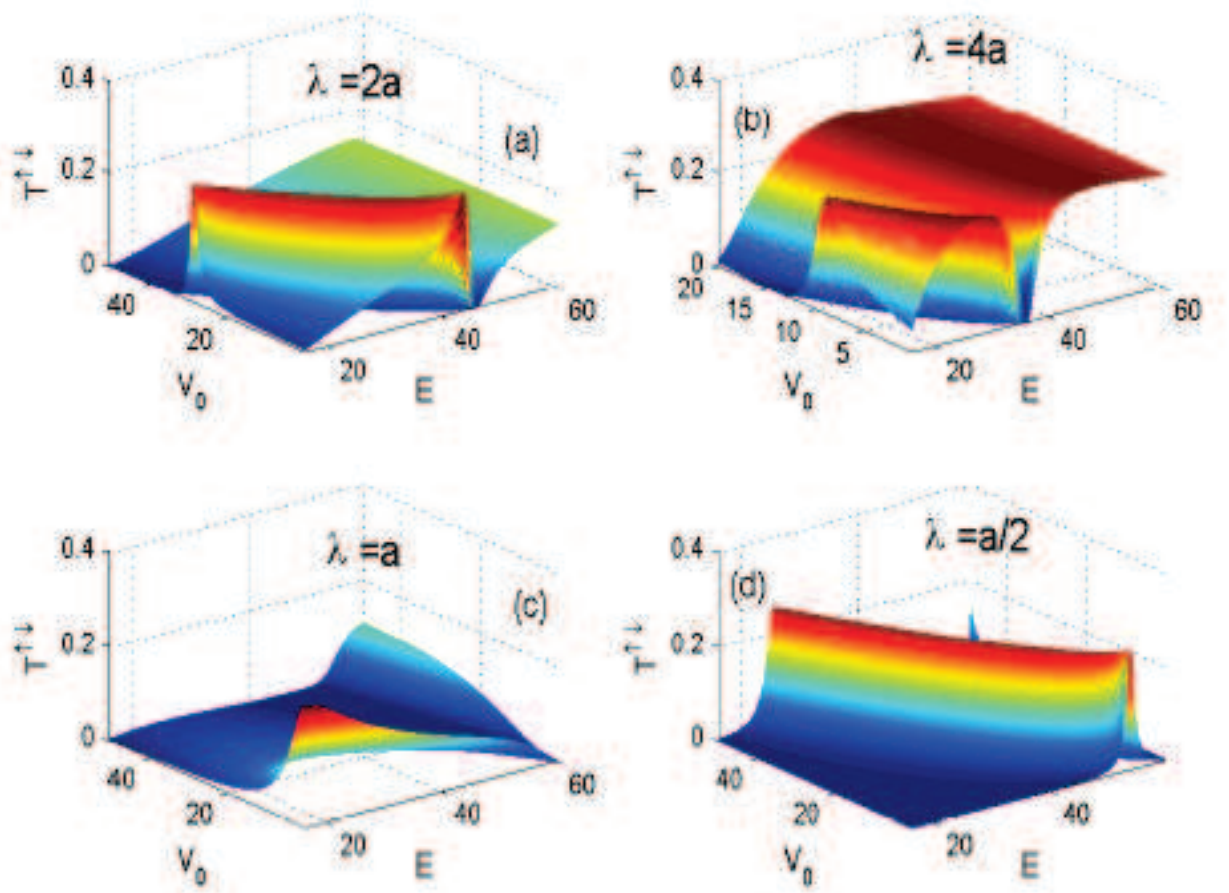


FIG. 3: Spin-flipped transmission $T^{\uparrow\downarrow}$ as a function of the incident energy E and the CCH well depth V_0 in the CCH-film-embedded quasi-1D electron waveguide. As in Fig 2, the four panels are for different λ and only the propagating subband is considered. Here, $T^{\uparrow\downarrow} = T^{\downarrow\uparrow}$.

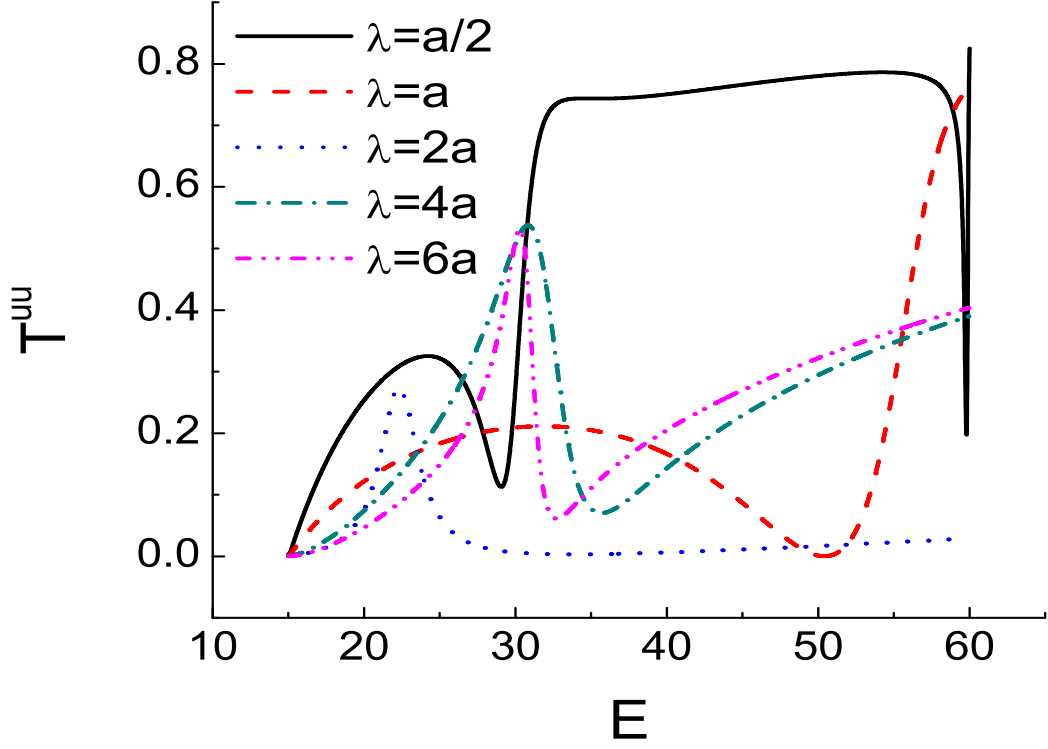


FIG. 4: Spin-conserved transmission $T^{\uparrow\uparrow}$ (T^{uu} in the figure) as a function of the incident energy E for different λ in the CCH-film-embedded quasi-1D electron waveguide. The CCH-well-depth $V_0 = 39$ meV for $\lambda = a/2$ and a ; $V_0 = 20$ meV for $\lambda = 2a$; and $V_0 = 1$ meV for $\lambda = 4a$ and $6a$. As in previous figures, only the propagating subband is considered. Also, $T^{\uparrow\uparrow} = T^{\downarrow\downarrow}$.

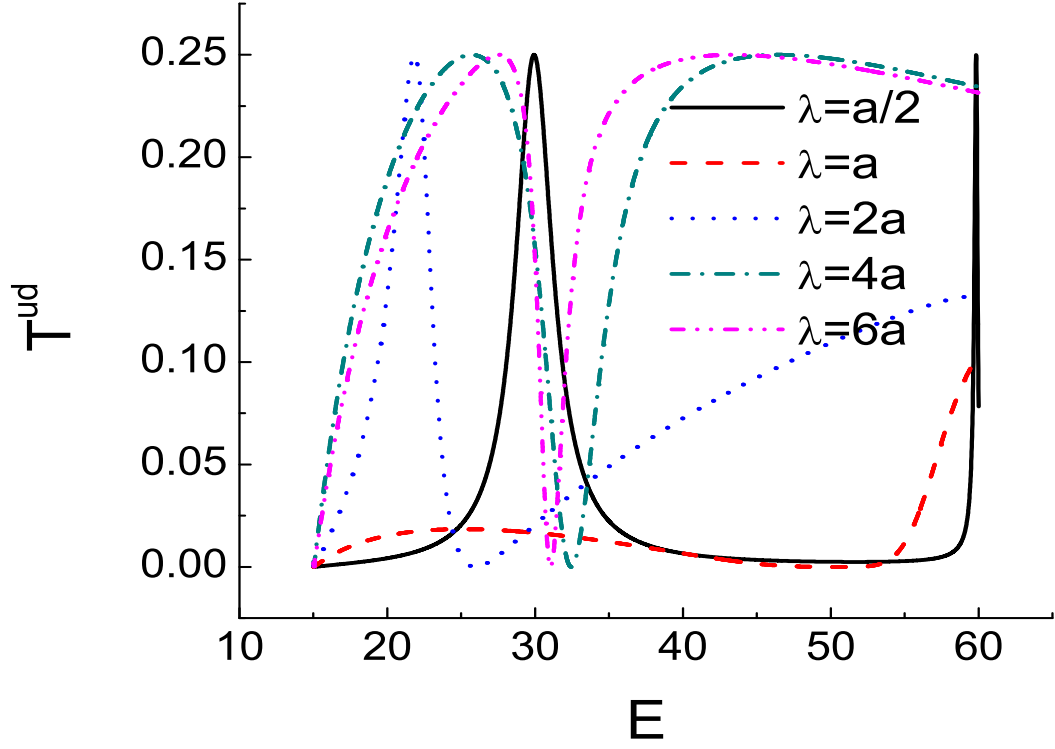


FIG. 5: Spin-flipped transmission $T^{\uparrow\downarrow}$ (T^{ud} in the figure) as a function of the incident energy E for different λ in the CCH-film-embedded quasi-1D electron waveguide. The CCH-well-depth V_0 is the same as Fig. 4. As in previous figures, only the propagating subband is considered. Also, $T^{\uparrow\downarrow} = T^{\downarrow\uparrow}$.

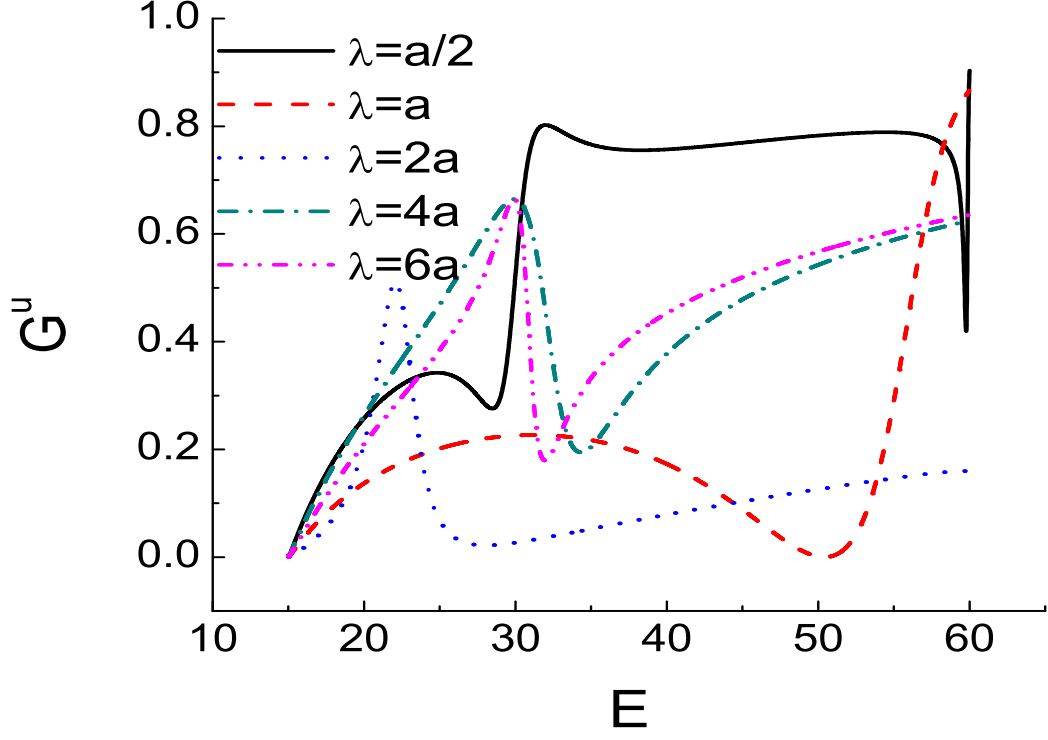


FIG. 6: Spin-up conductance G^\uparrow (G^u in the figure) as a function of the incident energy E for different λ in the CCH-film-embedded quasi-1D electron waveguide. Parameter settings are the same to Fig. 4. Also, $G^\uparrow = G^\downarrow$.